Prognostics of Remaining Useful Life for Lithium-Ion Batteries Based on Hybrid Approach of Linear Pattern Extraction and Nonlinear Relationship Mining

Yingzhou Wang, Chenyang Hei, Hui Liu, Shude Zhang, *Student Member, IEEE*, and Jianguo Wang

***Abstract*—The accurate prediction of the remaining useful life (RUL) of lithium-ion batteries (LIBs) is a key, challenging research direction. In this study, a battery degradation model is built based on the LIB dataset of NASA. A data decomposition prediction method, which extracts the linear trend from the capacity degradation data and then predicts the residuals of time series with nonlinear relations, is proposed. Then, an autoregressive integrated moving average-long short-term memory (ARIMA-LSTM) combined model for predicting the RUL of LIBs is established. The linear trend of capacity degradation is predicted by the ARIMA model and the LSTM model is established to predict the nonlinear residuals separated from the capacity degradation. The summation of both obtains the final battery RUL prediction result. Compared with the LSTM model and prediction models of similar types in existing literature in recent two years, the experimental results show that the RUL prediction error of the proposed model in this article is no more than one cycle, which is smaller than that of all the models involved in the comparison. Thus, this method has higher prediction accuracy and model generalization ability in the prediction of the remaining useful life of LIBs.**

***Index Terms*—Autoregressive integrated moving average-long short-term memory (ARIMA-LSTM) combined model, linear and nonlinear pattern decomposition, lithium-ion batteries (LIBs), remaining useful life (RUL).**

I. Introduction

LITHIUM-ION batteries (LIBs) have long service life, stable electrochemical performance, high energy density, and other excellent performances, which are widely used in electric vehicles, power grid energy storage system, and other fields [1], [2]. However, with the increase of charging and discharging times, the total capacity and power of the battery is degraded [3]. Battery failure prediction and health management has become a hot issue in battery health research at present [4], among which state of health (SOH) diagnosis and remaining useful life (RUL) prediction are the key technologies [5]. When battery capacity decays to 80% of rated capacity, the performance of the LIBs degrades, which may lead to catastrophic events [6]. Therefore, to maintain and replace batteries in time to avoid accidents, accurate RUL prediction becomes very important [7].

The RUL prediction methods of LIBs are generally divided into two categories: The first is the model-based method. Ramadass et al. [8] constructed an SOH attenuation model suitable for low-rate charge discharge by establishing a semiempirical expression for the anode-side reaction, coupling with the P2D model, and calculating the side reaction rate and solid electrolyte interphase (SEI) film internal resistance increment by using the Bulter Volmer kinetic equation. Dung et al. [9] combined the resistor-capacitance (RC) model with the Thevenin model, which considers the influence of nonlinear changes in battery capacity well and achieves a high accuracy. Clearly, the advantage of these model-based methods is that they can accurately model the battery capacity degradation model, but battery degradation has a complex internal mechanism and a nonlinear behavior [10], which makes balancing the complexity of the model and the accuracy of prediction difficult [11]. Therefore, the second kind of method, termed as data-driven method, is different from the model-based method and more practical. This method does not need to establish an accurate, complex physical model but only needs to mine the hidden feature information in the historical data to predict LIB RUL [12]. Zhou and Huang [13] proposed a battery RUL prediction method based on empirical mode decomposition (EMD) method and autoregressive integrated moving average (ARIMA) model. By comparing with relevance vector machine, monotonic echo sate networks, and ARIMA method, the potential of statistical analysis model for battery RUL prediction is demonstrated. Tong et al. [14] proposed the adaptive dropout long short-term memory method, which can effectively solve the overfitting problem of LSTM under the condition of small sample training data and has a good effect on the early prediction of battery RUL. Wang et al. [15] proposed

Manuscript received 25 January 2022; revised 22 April 2022; accepted 30 May 2022. Date of publication 13 June 2022; date of current version 10 October 2022. This work was supported by the Science and Technology Project of Jilin Province under Grant 20220508002RC. Recommended for publication by Associate Editor Sheldon Williamson. *(Corresponding author: Jianguo Wang.)*

Yingzhou Wang, Chenyang Hei, Shude Zhang, and Jianguo Wang are with the Jilin Province International Research Center of Precision Drive and Intelligent Control, Northeast Electric Power University, Jilin 132000, China (e-mail: wangyingzhou@ncepu.edu.cn; heichenyang429@163.com; shudezhang@outlook.com; wjg@neepu.edu.cn).

Hui Liu is with the State Grid Jibei Electric Power Research Institute (North China Electric Power Research Institute Co. Ltd), Beijing 100054, China (e-mail: liu.hui.c@jibei.sgcc.com.cn).

Color versions of one or more figures in this article are available at https://doi.org/10.1109/TPEL.2022.3182135.

Digital Object Identifier 10.1109/TPEL.2022.3182135

a support vector regression (SVR) method based on ant lion optimization (ALO) to predict the RUL of LIBs. In this method, ALO algorithm is used to optimize the kernel parameters of SVR, and the combination of the two could effectively improve prediction accuracy. In addition to the above studies, there are many excellent studies, which have solved many problems in data-driven prediction methods, such as long-term dependence, kernel parameter optimization, and feature variable expansion [16]–[18], but there are still shortcomings such as unsatisfactory long-term prediction performance and the need for large amount of high-quality historical data for training [13], [19]. Moreover, most of the existing literature only study from the perspective of nonlinear fluctuation feature of degradation data and objectively ignore the evident linear trend feature of degradation data.

To avoid the interference of large-scale linear trend when models learn nonlinear fluctuation features from the training data, and enable models to learn more useful feature information from a small sample data, this article proposes a data-processing method that decomposes the linear trend and the nonlinear residual in the data, and further recommends a data-driven RUL prediction method based on the ARIMA and long short-term memory (LSTM) combined model. This method can avoid the inadequate data utilization and amplify the scale of nonlinear fluctuation features. In this method, linear time-series prediction algorithm ARIMA is combined with deep neural network LSTM. The ARIMA algorithm, which is good at predicting short-term stationary time series, is used to extract the linear trend feature of the capacity degradation model and predict the linear part of the capacity degradation data. The LSTM algorithm, which is good at predicting nonlinear sequences, is used to study the long-term dependence between degraded battery capacity and predict the nonlinear residual part. The results of the two predictions are superposed to obtain the final prediction results. The proposed combinatorial method enables the model to capture the linear trend feature and nonlinear fluctuation feature of capacity degradation directly.

In this article, the proposed model is used to predict the RUL of B5, B6, B7, and B18 LIBs data in the NASA Ames Prognostics Center of Excellence dataset [20]. The accuracy and robustness of the proposed method are verified by comparison with existing literature models in recent two years. The rest of this article is organized as follows. Section II introduces the combined method and modeling process of the proposed model. Section III designs the RUL prediction comparison experiment of the ARIMA-LSTM combined model and the LSTM model. Section IV analyzes the results of the RUL prediction experiment and the comparative analysis. Section V concludes this article.

II. Model Establishment

A. ARIMA Model

ARIMA is a widely used time-series prediction model. It is a comprehensive algorithm that combines the autoregressive (AR) model, the moving average (MA) model, and differential processing [13]. Among them, AR(p) describes the relationship between the current value and the historical value of the sequence, and uses the historical data of the sequence to predict the sequence itself, which is expressed as follows:

$$x_t = \mu + \sum_{i=1}^{p} \gamma_i x_{t-i} + \epsilon_t \tag{1}$$

MA(q) represents the weighted sum of the error terms in the stationary time series, and the periodic window sliding is used to realize the smooth prediction of the future data. The details are as follows:

$$x_t = \mu + \epsilon_t + \sum_{i=1}^{q} \theta_i \epsilon_{t-i}. \tag{2}$$

The ARMA(p, q) model is composed of a linear combination of AR(p) and MA(q), which is expressed as follows:

$$x_t = \mu + \sum_{i=1}^{p} \gamma_i x_{t-i} + \epsilon_t + \sum_{i=1}^{q} \theta_i \epsilon_{t-i} \tag{3}$$

where x_t is the current value of the sequence, μ is the constant term of the equation, γ_i is the autocorrelation coefficient, ϵ_t is the regression error, and θ_i is the moving average parameter to be estimated.

B. LSTM Model

LSTM is an improved RNN model which transmits not only the hidden state but a cell state [21]. The cell state is an information storage unit made up of three door control structure, input, output, and forgotten door. This cell state transmitted can be understood as modification of memory state in long-term memory, filtering useless old information, and passing useful information to solve the long-term dependence problem. The calculation of LSTM can be divided into the following steps.

1) The current input information value of input gate $\tilde{c}_t$ is calculated, where W_c is the weight matrix, h_{t-1} is the state of the hidden layer at the previous moment, x_t is the input value at the current moment, and b_c is the bias item.

$$\tilde{c}_t = \tanh\left(W_c \cdot [h_{t-1}, x_t] + b_c\right). \tag{4}$$

2) The input ratio i_t of the input gate is calculated, where σ is the activation function Sigmoid function, W_i is the weight matrix, and b_i is the bias term.

$$i_t = \sigma\left(W_i \cdot [h_{t-1}, x_t] + b_i\right). \tag{5}$$

3) The forgetting ratio f_t of the forgetting gate is calculated, where W_f is the weight matrix, and b_f is the bias term.

$$f_t = \sigma\left(W_f \cdot [h_{t-1}, x_t] + b_f\right). \tag{6}$$

4) The memory cell storage value c_t is calculated, where c_{t-1} is the storage value at the previous moment of the storage unit.

$$c_t = f_t * c_{t-1} + i_t * \tilde{c}_t. \tag{7}$$

5) The output ratio of output gate o_t is calculated, where W_o is the weight matrix, and b_o is the bias term.

$$o_t = \sigma\left(W_o \cdot [h_{t-1}, x_t] + b_o\right). \tag{8}$$

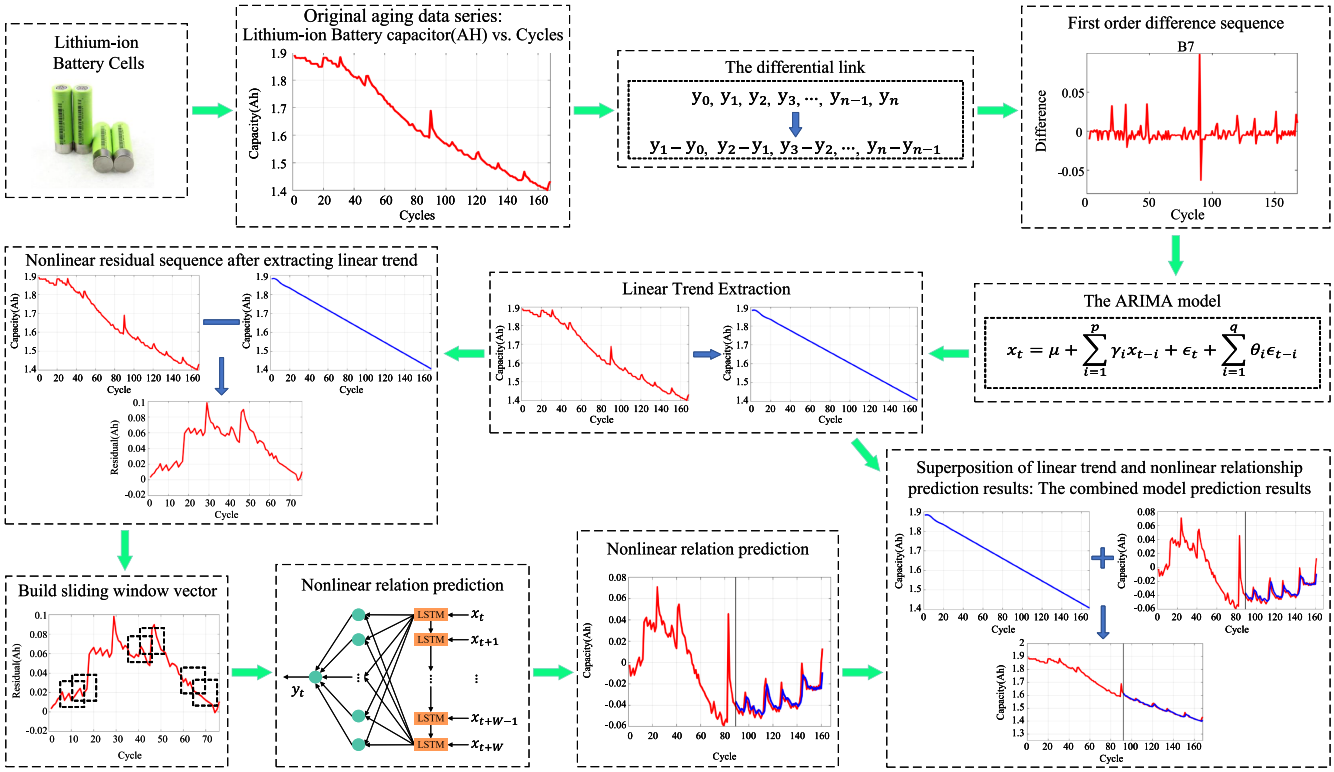

Fig. 1. Schematic diagram of combined forecasting method based on linear pattern extraction and nonlinear relation mining.

6) Output value h_t is calculated.

$$h_t = o_t * \tanh(c_t). \tag{9}$$

The LSTM model constructed is suitable for modeling and describing the long- and short-term nonlinear data.

C. ARIMA-LSTM Combined Model

The schematic diagram of combined forecasting method proposed in this article is shown in Fig. 1 (all the curves in Fig. 1 are from a prediction experiment using 55% B7 battery capacity degradation data as training set). Based on the main idea that decomposes the linear part and the nonlinear part of the capacity degradation data and then predicts both separately, the ARIMA-LSTM combined model for RUL prediction of LIBs is built. The ARIMA model is used to predict the linear trend of the input sample sequence, and the LSTM model is used to predict the nonlinear residual separated from the battery capacity degradation data. The two capacity prediction data are added to obtain the final capacity prediction data, thereby predicting the RUL of the battery. The ARIMA-LSTM modeling is as follows.

1) *Data preprocessing and stability analysis:* Perform D-order difference on the data until the data is stable.
2) *Order determination of ARIMA model:* After the data become stable, the order is determined by the grid search method, based on the evaluation indexes of Akaike information criterion (AIC) and Bayesian information criterion (BIC).
3) *Independence test:* The Durbin–Watson method is used to test the independence of the fitted residual sequence of the training set of the ARIMA model after the grading.
4) *Sliding-window vector matrix construction:* The linear trend prediction value generated by the ARIMA model prediction and the real capacity value are made a difference and construct the sliding-window vector matrix.
5) *LSTM model training:* The error in training is minimized, and the learning rate is automatically optimized through the adaptive moment estimation (Adam) optimizer until the training ends after reaching the epoch numbers.
6) *RUL prediction:* The model after training is used to predict the test set, and the predicted results are superimposed with the linear trend predicted values of the ARIMA model as the final capacity predicted value.

The flow chart of combined model is shown in Fig. 2 and the block diagram of entire framework is shown in Fig. 3. The algorithm of ARIMA-LSTM combined model is described as Algorithm 1.

III. RUL Prediction Experiment

A. Dataset Preparation

The experiment mainly uses the data of B5, B6, B7, and B18 batteries in the NASA Ames Prognostics Center of Excellence. The four batteries are 18650 LIBs with a capacity of 2 Ah. The four groups of LIBs are charged in constant current mode of 1.5 A at the same room temperature (24 °C) until the battery voltage reaches 4.2 V, and then switched to constant voltage

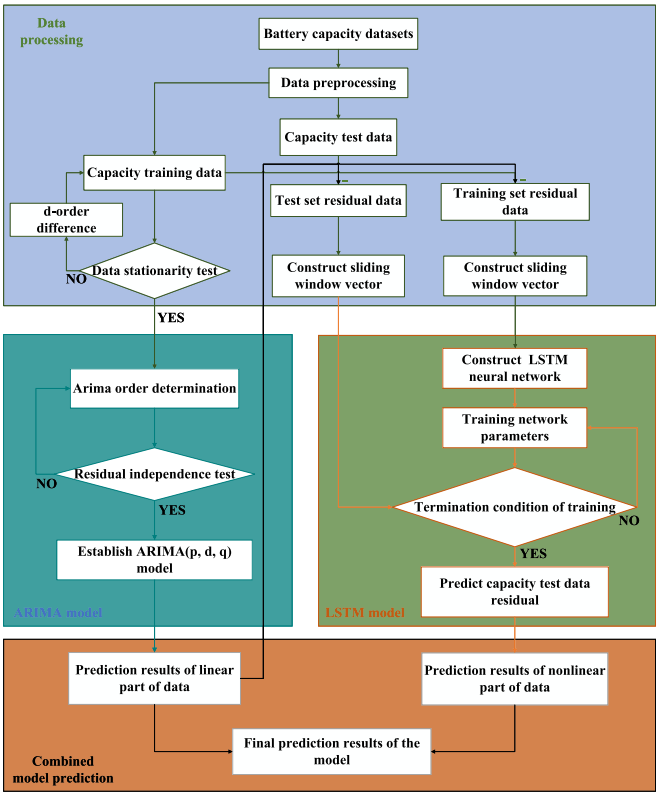

Fig. 2. Flow chart of ARIMA and LSTM combined model for predicting capacity and RUL of lithium-ion battery.

Algorithm 1: ARIMA-LSTM Combined Model.

Input: datasets as data
Output: predicted data as F^*
while all data which should been trained **do**
/*ARIMA model*/
Let G be the grid search matrix
for all $p, d, q \in G$ **do**
order $\leftarrow$ select_ic;
end for
Let T1 be the ARIAM train model;
T1 $\leftarrow$ ARIMA(data, order).fit;
Let L be the linear trend prediction results;
$L \leftarrow$ T1.predict;
/*LSTM model*/
Let S be the set of Data Index and R be the residual between source data and linear trend data;
for all $s \in S$ in the given sequence **do**
Windows[s] $\leftarrow$ R[s,..., s + windows_size];
Object[s] $\leftarrow$ R[s,..., s + windows_size];
end for
Let T2 be the LSTM train model;
T2 $\leftarrow$ LSTM(Windows, Obeject).train;
Let N be the nonlinear residual prediction results;
$N \leftarrow$ T2.predict;
Let F^* be the final prediction result of the combined model;
$F^* \leftarrow N + L$;
end while

mode to continue charging until the charging current drops below 20 mA. The test is to discharge at a constant current mode of 2 A until the voltages of B5, B6, B7, and B18 drop to 2.7, 2.5, 2.2, and 2.5 V, respectively. When the rated capacity of batteries decays by 30%, the end-of-life (EOL) criteria is reached, and then the experiment is stopped. The capacity degradation curve of the dataset is shown in Fig. 4. The details of the experimental dataset are shown in Table I.

TABLE I
DETAILS OF EXPERIMENTAL DATASET

No.	Temperature (°C)	Discharge current (A)	Capacity (Ah)	Cutoff voltage (V)
B5	24	2	2	2.7
B6	24	2	2	2.5
B7	24	2	2	2.2
B18	24	2	2	2.5

B. Evaluation Standard

This article uses mean absolute error (MAE) and root-mean-square error (RMSE) to evaluate the the accuracy of the model for LIBs RUL, and their expressions are as follows:

$$MAE = \frac{1}{N}\sum_{n=1}^{N}|X(n) - \hat{X}(n)| \tag{10}$$

$$RMSE = \sqrt{\frac{1}{N}\sum_{n=1}^{N}|X(n) - \hat{X}(n)|^2} \tag{11}$$

where $X(n)$ and $\hat{X}(n)$ represent the true value and predicted value sequence of battery capacity data, respectively; and N is the number of cycles between the first predicted cycle and the actual battery EOL.

E_r and PE_r are used to evaluate the prediction effect of the model RUL, their expressions are as follows:

$$E_r = |\text{PRUL} - \text{RUL}| \tag{12}$$

$$PE_r = \frac{|\text{PRUL} - \text{RUL}|}{\text{RUL}} \times 100\% \tag{13}$$

where RUL and PRUL are the absolute difference between the number of cycles when the system capacity and predicted capacity reach the EOL threshold and the number of cycles at the beginning of prediction. E_r represents the absolute error between RUL and PRUL, and PE_r represents the relative error between RUL and PRUL.

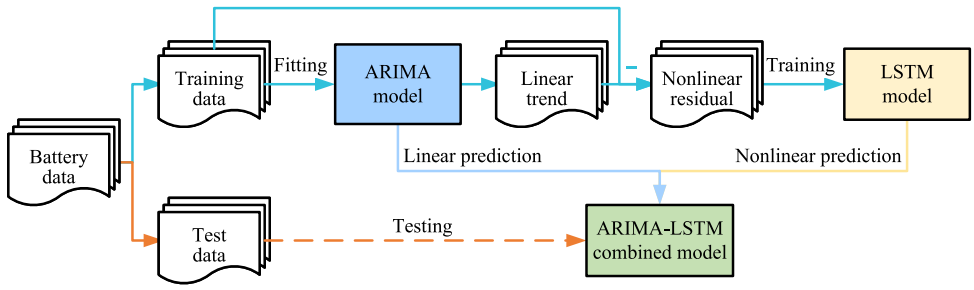

Fig. 3. Block diagram of entire framework.

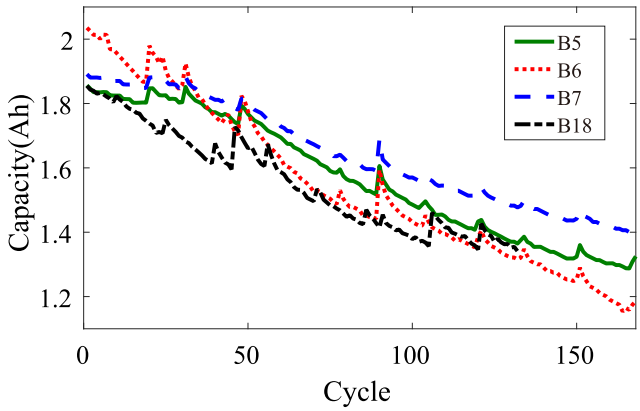

Fig. 4. Battery capacity degradation data.

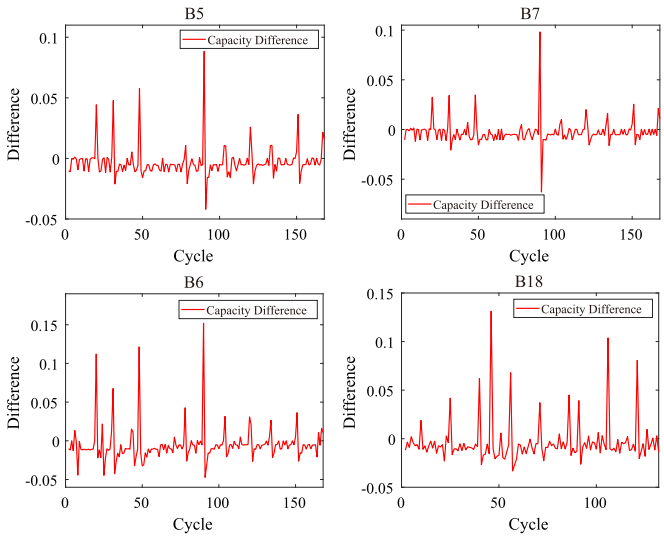

Fig. 5. First-order difference diagram of the dataset of battery models B5, B6, B7, and B18.

C. Experimental Design of RUL Prediction

The first-order difference is performed on their dataset based on the input of the model, and the data sequence after the difference is shown in Fig. 5. The figure shows that the corresponding data series of all batteries fluctuates around the constant 0, which belongs to a stationary time-series, after the first-order difference of the capacity training data. Meanwhile, the parameter d of the ARIMA(p, d, q) model is obtained according to the difference times: $d = 1$.

After the input data sequence of the model become stable, the order of the ARIMA(p, d, q) model is needed to obtain the AR order p and moving average q of the model. AIC and BIC criteria are used to determine the order of ARIMA model. The AIC and BIC of a given ARIMA(p, d, q) model can be expressed as follows:

$$AIC = 2k - 2\ln(L) \tag{14}$$

$$BIC = k\ln(n) - 2\ln(L) \tag{15}$$

where k is the number of model parameters, n is the total number of samples, and L is the likelihood estimation function.

Based on the grid search method, a pair of optimal p and q, which can calculate the minimum AIC or BIC values of the model, is determined as parameters in ARIMA (p, d, q):

$$\text{AIC}(\hat{p}, \hat{q}) = \min_{0\le p\le P, 0\le q\le Q} \text{AIC}(p, q) \tag{16}$$

$$\text{BIC}(\hat{p}, \hat{q}) = \min_{0\le p\le P, 0\le q\le Q} \text{BIC}(p, q). \tag{17}$$

The ARIMA model after determining the order needs to be tested for the independence of the fitting residuals to verify the rationality of the model. Dubin–Watson (DW) test method is used to test the independence of residuals, and the formula is as follows:

$$\text{DW} = \frac{\sum_{t=2}^{n}(e_t - e_{t-1})^2}{\sum_{t=1}^{n} e_t^2} \tag{18}$$

where e_t^2 is the fitting residual of the model. When the calculated value DW is within the range of $(d_u, 4 - d_u)$, the residual data sequence is considered an independent sequence. The value of d_u is determined by checking "Durbin–Watson tables," according to sample size and variable dimensions. The number of independent variables in the model is 1, the sample size of B5, B6, and B7 under the 45% training set is 76, and B18 is 59. According to the table, when significance level $\alpha = 0.05$, the range of calculated values DW for B5, B6, and B7 is (1.652, 2.348), and for B18 is (1.601, 2.399). Under the 55% training set, the sample size of B5, B6, and B7 is 92, and that of B18 is 73, and the range of calculated values DW for B5, B6, and B7 is (1.679, 2.321), and for B18 is (1.641, 2.359).

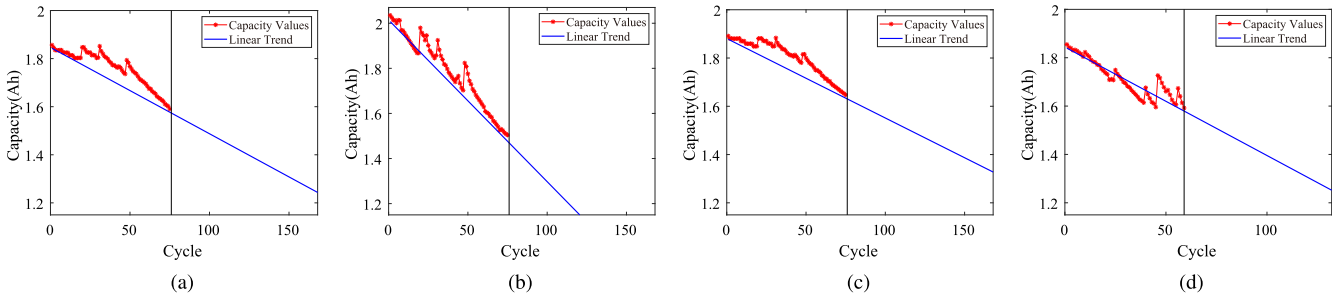

Fig. 6. Linear trend extraction based on ARIMA model using 45% data of total cycle as the training samples. (a) B5. (b) B6. (c) B7. (d) B18.

TABLE II
PARAMETER TABLE OF ARIMA-LSTM AND LSTM EXPERIMENT IN 45% TRAINING SET

Model	No.	ST	(p,d,q)	Epochs	Loss	Batch	EOL	Units
ARIMA -LSTM	B5	76	(1,1,0)	100	MSE	2	70%	20
	B6	76	(2,1,0)	100	MSE	1	70%	20
	B7	76	(1,1,0)	100	MSE	2	75%	20
	B18	59	(1,1,0)	100	MSE	2	70%	20
LSTM	B5	76	–	100	MSE	1	70%	30
	B6	76	–	100	MSE	1	70%	30
	B7	76	–	100	MSE	1	75%	30
	B18	59	–	100	MSE	1	70%	30

TABLE III
PARAMETER TABLE OF ARIMA-LSTM AND LSTM EXPERIMENT IN 55% TRAINING SET

Model	No.	ST	(p,d,q)	Epochs	Loss	Batch	EOL	Units
ARIMA -LSTM	B5	92	(2,1,0)	100	MSE	1	70%	20
	B6	92	(2,1,0)	100	MSE	2	70%	20
	B7	92	(3,1,2)	100	MSE	2	75%	20
	B18	73	(1,1,2)	100	MSE	2	70%	20
LSTM	B5	92	–	100	MSE	1	70%	30
	B6	92	–	100	MSE	1	70%	30
	B7	92	–	100	MSE	1	75%	30
	B18	73	–	100	MSE	1	70%	30

The validated ARIMA model outputs a linear trend prediction sequence of battery capacity data, which is compared with the capacity degradation training dataset to obtain a residual data training set of battery capacity degradation, that is, a nonlinear fluctuation feature training set. Mean square error [MSE, (19)] is used as the loss function of model training, and the Adam optimization method is used to optimize the model parameters and learning rate. The EOL of B5, B6, and B18 batteries for RUL prediction is 1.4 Ah (SOH=70%); 1.5 Ah (SOH=75%) is selected as the EOL of B7 because the capacity degradation data of B7 battery is not less than 1.4 Ah after all cycles. An LSTM model is introduced, and the same prediction starting point as the ARIMA-LSTM combined model is adopted. After optimizing the remaining network superparameters in the same number of iterations, the RUL of LIBs is predicted and compared with the proposed model. The parameter selection results of the ARIMA model and the superparameter settings of the LSTM network

TABLE IV
COMPARISON OF PREDICTION RESULTS BETWEEN ARIMA-LSTM AND LSTM FOR RUL PREDICTION USING 45% DATA OF THE TOTAL CYCLE AS THE TRAINING SAMPLES

Model	No.	ST	RUL	PRUL	E_r	PE_r%	MAE	RMSE
ARIMA -LSTM	B5	76	49	50	1	2.04%	0.0079	0.0132
	B6	76	33	27	6	18.18%	0.0303	0.0370
	B7	76	50	51	1	2.00%	0.0066	0.0133
	B18	59	38	39	1	2.63%	0.0161	0.0230
LSTM	B5	76	49	53	4	8.16%	0.0318	0.0395
	B6	76	33	35	2	6.06%	0.0226	0.0314
	B7	76	50	52	2	4.00%	0.0239	0.0344
	B18	59	38	–	–	–	0.1040	0.1110

model are shown in Tables II and III.

$$\text{MSE} = \frac{1}{N}\sum_{n=1}^{N}(X(n) - \hat{X}(n))^2. \tag{19}$$

IV. ANALYSIS OF EXPERIMENTAL RESULTS OF RUL PREDICTION

The experimental results of capacity linear trend prediction of the ARIMA model using 45% data of total cycle as the training samples are shown in Fig. 6. The capacity nonlinear residuals after extracting linear trend are shown in Fig. 7. The results of RUL prediction based on ARIMA-LSTM and LSTM using 45% data of the total cycle as the training samples are shown in Fig. 8, and their absolute estimation errors are shown in Fig. 9. According to the capacity prediction curves, the prediction curves of ARIMA-LSTM combined model are more consistent with the real data curves (the black curves), and the model performs well in the prediction. Table IV presents the RUL prediction results and model accuracy of the ARIMA-LSTM combined model and the LSTM model using 45% data of the total cycle as the training samples. The predicted results and model accuracy of B5, B7, and B18 are significantly better than that of the LSTM model. The E_r predicted by RUL of B5 battery under the LSTM model is four cycles, whereas the E_r predicted by RUL of B5 battery under the ARIMA-LSTM combined model is one cycle. Under the LSTM model, the predicted value of the capacity of the B18 battery will not drop to the failure threshold; hence, it is expressed with "–." Under the combined model, the forecast error of RUL is only one cycle. In terms

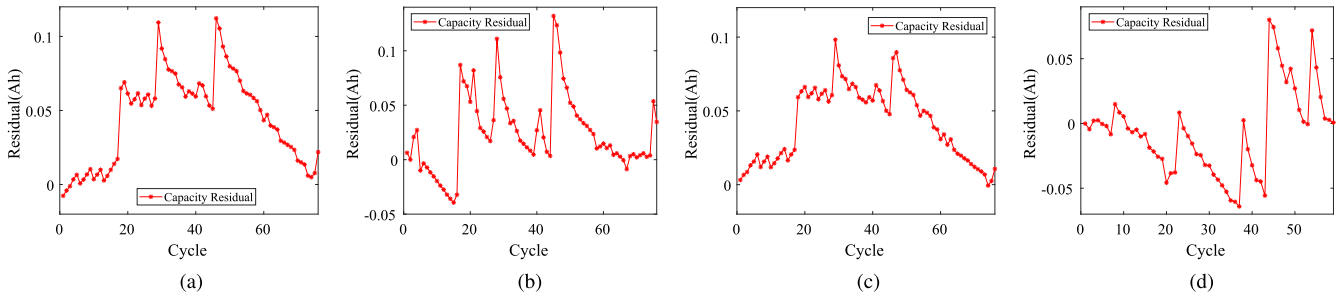

Fig. 7. Capacity nonlinear residual after extracting linear trend using 45% data of the total cycle as the training samples. (a) B5. (b) B6. (c) B7. (d) B18.

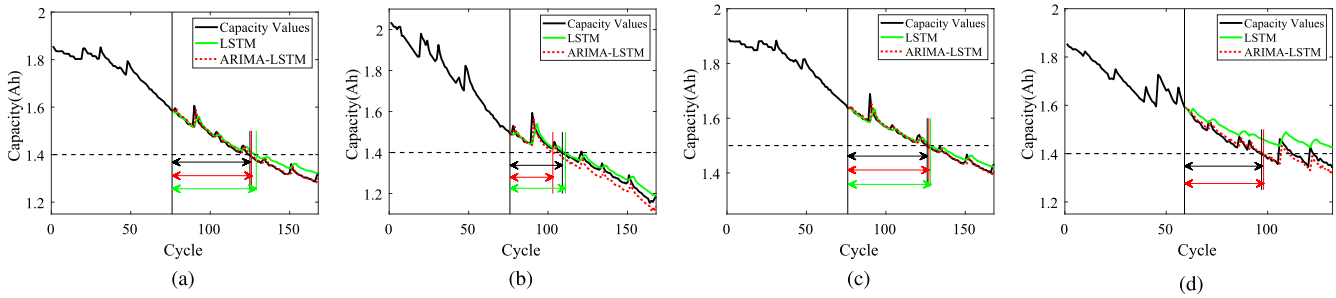

Fig. 8. Results of RUL prediction based on ARIMA-LSTM and LSTM using 45% data of the total cycle as the training samples. (a) B5. (b) B6. (c) B7. (d) B18.

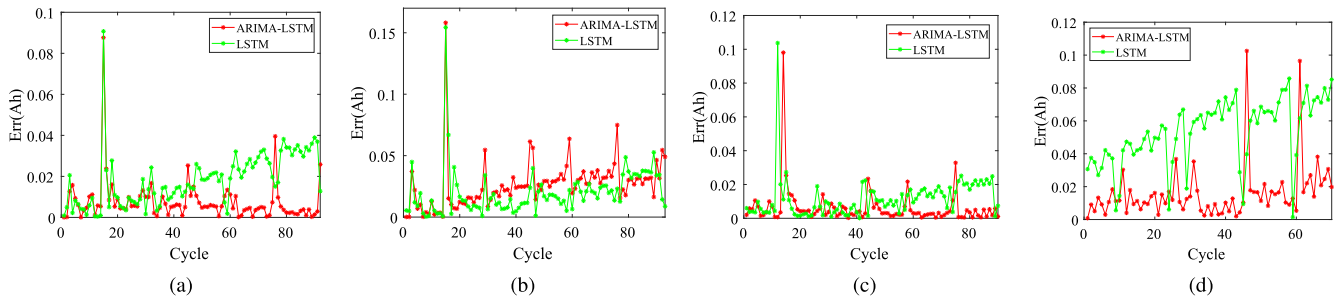

Fig. 9. Absolute estimation errors of ARIMA-LSTM and LSTM used in RUL prediction using 45% data of the total cycle as the training samples. (a) B5. (b) B6. (c) B7. (d) B18.

of model accuracy, taking B5 as an example, the MAE of the LSTM model is 0.0318, and RMSE is 0.0395, whereas the MAE value of the ARIMA-LSTM combined model is only 0.0079, and RMSE is only 0.0132. The prediction accuracy of the other battery models under the combined model is also significantly better than that of the LSTM model. The RUL forecast error and model accuracy of B6 battery are slightly worse than those of the LSTM model. However, experiments reveal that the predicted results of the combined model are very stable, whereas the prediction results of the LSTM model fluctuate greatly. Thus, the robustness of the combined model is better than that of the LSTM model.

The ARIMA linear trend prediction is shown in Fig. 10, and the prediction residual of the ARIMA model under the 55% training set is shown in Fig. 11. The battery RUL prediction experimental results of the ARIMA-LSTM combined model using 55% data of the total cycle as the training samples are shown in Fig. 12, and their absolute estimation errors are shown in Fig. 13. According to the capacity prediction curves, the RUL prediction accuracy of the ARIMA-LSTM combined model is higher than that of the LSTM model, and the prediction results are closer with the real values (the black curves). Table V presents the RUL prediction results and model accuracy of the ARIMA-LSTM combined model and the separate LSTM model with 55% training data. The RUL prediction results and model accuracy of the ARIMA-LSTM combined model are comprehensively superior. RUL predicts E_r for B6 batteries is zero cycles, RUL predicts E_r for B5, B7, and B18 batteries is all one cycle, the predicted MAE of B5 and B7 batteries is 0.0065 and 0.0049, respectively, and RMSE values are 0.0092 and 0.0078, respectively. The MAE values of B5 and B7 batteries under the LSTM model are 0.0484 and 0.0453, respectively, and RMSE values are 0.0541 and 0.0512, respectively. The model accuracy of B6 and B18 batteries under the combined model is

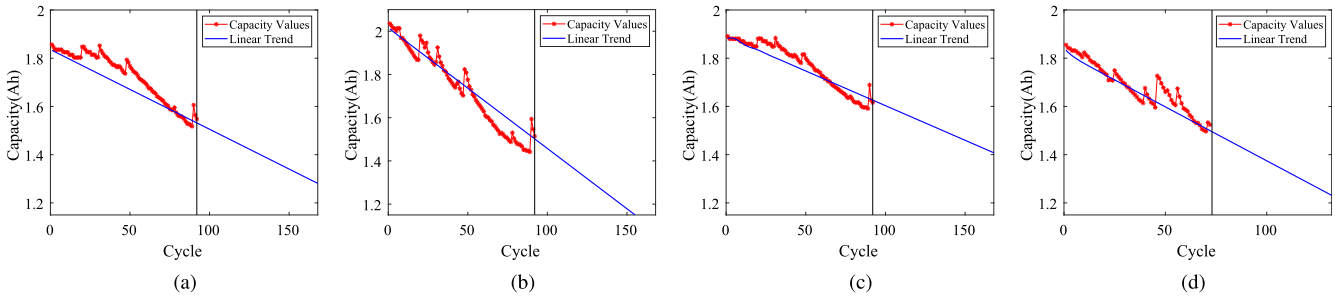

Fig. 10. Linear trend extraction based on ARIMA model using 55% data of total cycle as the training samples. (a) B5. (b) B6. (c) B7. (d) B18.

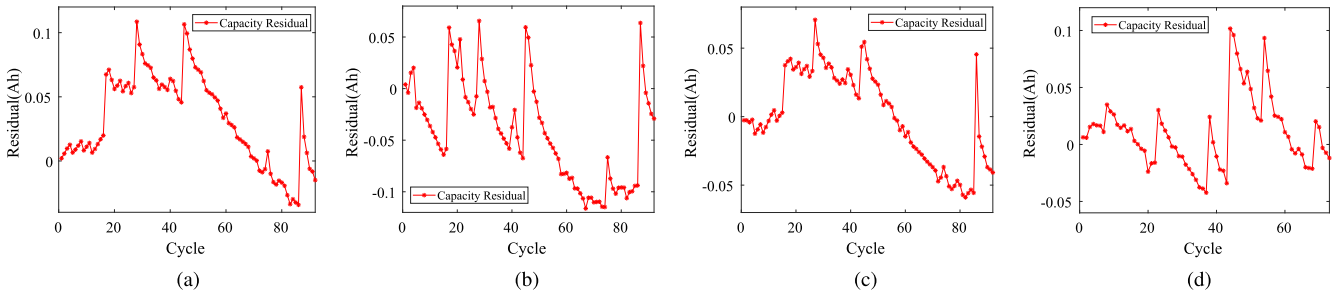

Fig. 11. Capacity nonlinear residual after extracting linear trend using 55% data of the total cycle as the training samples. (a) B5. (b) B6. (c) B7. (d) B18.

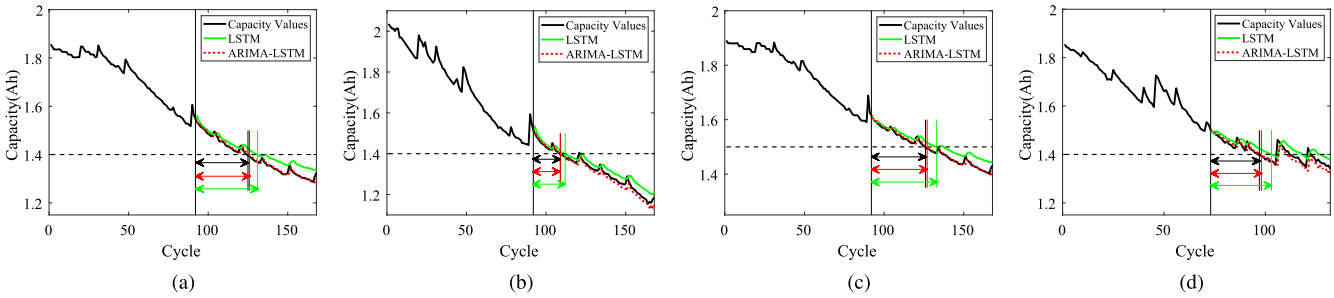

Fig. 12. Results of RUL prediction based on ARIMA-LSTM and LSTM using 55% data of the total cycle as the training samples. (a) B5. (b) B6. (c) B7. (d) B18.

TABLE V
COMPARISON OF PREDICTION RESULTS BETWEEN ARIMA-LSTM AND LSTM FOR RUL PREDICTION USING 55% DATA OF THE TOTAL CYCLE AS THE TRAINING SAMPLES

Model	No.	ST	RUL	PRUL	E_r	PE_r%	MAE	RMSE
ARIMA -LSTM	B5	92	33	34	1	3.03%	0.0065	0.0092
	B6	92	17	17	0	0.00%	0.0129	0.0174
	B7	92	34	35	1	2.94%	0.0049	0.0078
	B18	73	24	25	1	4.17%	0.0149	0.0233
LSTM	B5	92	33	39	6	18.18%	0.0484	0.0541
	B6	92	17	20	3	17.65%	0.0291	0.0321
	B7	92	34	41	7	20.59%	0.0453	0.0512
	B18	73	24	30	6	25.00%	0.0534	0.0570

also significantly better than that of the LSTM model. Thus, the prediction performance of the ARIMA-LSTM combined model is significantly better than that of the LSTM model.

To verify the performance of the proposed model further, the predicted results of proposed model are compared with that of models in the existing studies which are similar in type under the same conditions. Table VI presents the RUL prediction results and evaluation indices of the ARIMA-LSTM combined model with 45% and 55% training data and the models in the existing literature.

The ARIMA model used in [13] and the EMD-ARIMA model proposed in [13] are compared to verify that the proposed model is superior to autoregressive models. The multichannel LSTM model proposed in [16] and the LSTM network model combining particle swarm optimization and attention mechanism (PA-LSTM) proposed in [22] are compared to verify that the proposed method is superior to other improved LSTM algorithms. The method of combining adaptive unscented Kalman filter and genetic algorithm optimized support vector regression (AUKF-GA-SVR) proposed in [17] and the method of combining relevance vector machine and gray model (RVM-GM) proposed

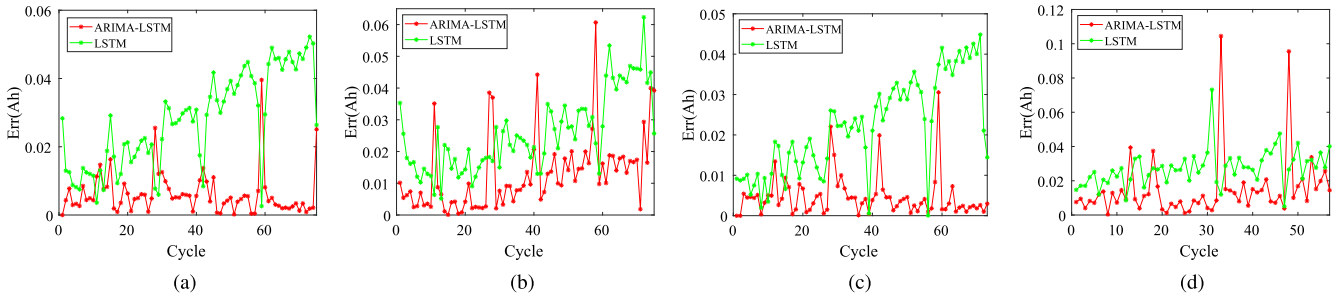

Fig. 13. Absolute estimation errors of ARIMA-LSTM and LSTM used in RUL prediction using 55% data of the total cycle as the training samples. (a) B5. (b) B6. (c) B7. (d) B18.

TABLE VI
COMPARISON OF PREDICTION RESULTS BETWEEN ARIMA-LSTM AND OTHER RUL MODELS

No.	Model	ST	E_r	MAE	RMSE
B5	**ARIMA-LSTM**	**76**	**1**	**0.0079**	**0.0132**
	ARIMA [13]	80	16	–	0.0214
	AUKF-GA-SVR [17]	80	3	0.0125	0.0192
	PA-LSTM [22]	90	3	–	0.0166
	EMD-ARIMA [13]	90	13	–	0.0195
	ARIMA-LSTM	**92**	**1**	**0.0065**	**0.0092**
	MC-LSTM [16]	100	–	0.0181	0.0208
B6	**ARIMA-LSTM**	**76**	**6**	**0.0303**	**0.0370**
	ARIMA [13]	80	16	–	0.0382
	AUKF-GA-SVR [17]	80	7	0.0368	0.0483
	RVM-GM [23]	80	15	–	0.0307
	PA-LSTM [22]	90	11	–	0.0293
	EMD-ARIMA [13]	90	0	–	0.0285
	ARIMA-LSTM	**92**	**0**	**0.0129**	**0.0174**
	MC-LSTM [16]	100	–	0.0299	0.0428
B7	**ARIMA-LSTM**	**76**	**1**	**0.0066**	**0.0133**
	AUKF-GA-SVR [17]	80	0	0.0089	0.0124
	RVM-GM [23]	80	7	–	0.0119
	ARIMA [13]	90	167	–	–
	EMD-ARIMA [13]	90	2	–	0.0113
	ARIMA-LSTM	**92**	**1**	**0.0049**	**0.0078**
	MC-LSTM [16]	100	–	0.0190	0.0231
B18	**ARIMA-LSTM**	**59**	**1**	**0.0161**	**0.0230**
	AUKF-GA-SVR [17]	60	4	0.0121	0.0233
	PA-LSTM [22]	70	8	–	0.0287
	ARIMA-LSTM	**73**	**1**	**0.0149**	**0.0233**
	MC-LSTM [16]	79	–	0.0393	0.0449

in [23] are compared to verify that the method proposed in this article is superior to other machine learning models. To ensure the rationality of the comparison, the prediction starting points of all the compared models are close to the proposed model. The predicted E_r values of the models in the existing literature are all larger than the predicted E_r values of the models proposed in this article to varying degrees (the "–" in the table indicates that the evaluation index has not been verified in the literature where the model is located). Taking B5 as an example, the E_r of the proposed model is equal to one cycle at different prediction starting points, whereas the E_r of the AUKF-GA-SVR and PA-LSTM models is three cycles, which is greater than that of the proposed model. Therefore, the prediction effect of the model proposed in this article, which can more accurately predict the RUL of LIBs, is better than that of the methods in the existing literature. Moreover, the MAE and RMSE of the prediction method proposed in this article are smaller than those in the existing literature.

V. CONCLUSION

This article proposes a method to decompose the linear pattern and nonlinear relationship in capacity degradation data, and the ARIMA-LSTM combined model is constructed to predict the RUL of LIBs based on the proposed method, using the ARIMA method to predict the linear trend of capacity data in advance in multiple steps and LSTM to predict the nonlinear capacity residuals gradually. The main contributions of this article are as follows.

1) According to the characteristics of battery capacity degradation data, a novel data decomposition and prediction method for battery RUL prediction is proposed. By the decomposition of linear pattern and nonlinear relationship, the original capacity degradation sequence is decomposed into two independent sequences. It can overcome the interference of large-scale linear trend when models learn nonlinear fluctuation features in the training data, which makes the model learn the entire degradation trend and nonlinear fluctuation feature more efficiently.
2) Based on the proposed data decomposition and prediction method, a novel battery RUL prediction algorithm is proposed, the corresponding ARIMA-LSTM combination model is constructed, the ARIMA automatic order determination of the combined model in the process of prediction is solved, and the accurate battery RUL prediction is achieved.
3) The proposed model has an excellent performance in the small sample data prediction of battery RUL and the reduction of error accumulation, as well as prominent online prediction ability. In all experiments, MAE of the proposed model decreased by 0.0323 on average compared with LSTM model. Moreover, the proposed model has a faster convergence and a stronger robustness.

4) The proposed model has good generalization ability and performs satisfactory prediction effect for all the four batteries, especially for the battery capacity degradation data with large nonlinear fluctuations such as B18 battery. In the experiment, the cycle errors of the predicted results are not more than one cycle, and MAE is less than 0.017.

REFERENCES

[1] R. Jiao, K. Peng, and J. Dong, "Remaining useful life prediction of lithium-ion batteries based on conditional variational autoencoders-particle filter," *IEEE Trans. Instrum. Meas.*, vol. 69, no. 11, pp. 8831–8843, Nov. 2020.

[2] Y. Zhang, R. Xiong, H. He, and W. Shen, "Lithium-ion battery pack state of charge and state of energy estimation algorithms using a hardware-in-the-loop validation," *IEEE Trans. Power Electron.*, vol. 32, no. 6, pp. 4421–4431, Jun. 2016.

[3] T. Sun *et al.*, "A novel hybrid prognostic approach for remaining useful life estimation of lithium-ion batteries," *Energies*, vol. 12, no. 19, p. 3678, 2019, doi: 10.3390/en12193678.

[4] A. Kara, "A data-driven approach based on deep neural networks for lithium-ion battery prognostics," *Neural Comput. Appl.*, vol. 33, no. 20, pp. 13525–13538, Oct. 2021.

[5] G. Dong, F. Yang, Z. Wei, J. Wei, and K.-L. Tsui, "Data-driven battery health prognosis using adaptive Brownian motion model," *IEEE Trans. Ind. Inform.*, vol. 16, no. 7, pp. 4736–4746, Jul. 2019.

[6] X. Hu, L. Xu, X. Lin, and M. Pecht, "Battery lifetime prognostics," *Joule*, vol. 4, no. 2, pp. 310–346, 2020.

[7] L. Ren, J. Dong, X. Wang, Z. Meng, L. Zhao, and M. J. Deen, "A data-driven Auto-CNN-LSTM prediction model for lithium-ion battery remaining useful life," *IEEE Trans. Ind. Inform.*, vol. 17, no. 5, pp. 3478–3487, May 2020.

[8] P. Ramadass, B. Haran, P. M. Gomadam, R. White, and B. N. Popov, "Development of first principles capacity fade model for Li-ion cells," *J. Electrochem. Soc.*, vol. 151, no. 2, p. A196, 2004, doi: 10.1149/1.1634273.

[9] L.-R. Dung, H.-F. Yuan, J.-H. Yen, C.-H. She, and M.-H. Lee, "A lithium-ion battery simulator based on a diffusion and switching overpotential hybrid model for dynamic discharging behavior and runtime predictions," *Energies*, vol. 9, no. 1, p. 51, 2016, doi: 10.3390/en9010051.

[10] K. Liu, Y. Shang, Q. Ouyang, and W. D. Widanage, "A data-driven approach with uncertainty quantification for predicting future capacities and remaining useful life of lithium-ion battery," *IEEE Trans. Ind. Electron.*, vol. 68, no. 4, pp. 3170–3180, Apr. 2020.

[11] G. Dong, Z. Chen, J. Wei, and Q. Ling, "Battery health prognosis using Brownian motion modeling and particle filtering," *IEEE Trans. Ind. Electron.*, vol. 65, no. 11, pp. 8646–8655, Nov. 2018.

[12] S. Wang, L. Zhao, X. Su, and P. Ma, "Prognostics of lithium-ion batteries based on flexible support vector regression," in *Proc. Prognostics Syst. Health Manage. Conf.*, 2014, pp. 317–322.

[13] Y. Zhou and M. Huang, "Lithium-ion batteries remaining useful life prediction based on a mixture of empirical mode decomposition and ARIMA model," *Microelectronics Rel.*, vol. 65, pp. 265–273, 2016.

[14] Z. Tong, J. Miao, S. Tong, and Y. Lu, "Early prediction of remaining useful life for lithium-ion batteries based on a hybrid machine learning method," *J. Cleaner Prod.*, vol. 317, 2021, Art. no. 128265.

[15] Y. Wang, Y. Ni, Y. Zheng, X. Shi, and J. Wang, "Remaining useful life prediction of lithium-ion batteries based on support vector regression optimized and ant lion optimizations," *Zhongguo Dianji Gongcheng Xuebao/Proceedings Chin. Soc. Elect. Eng.*, vol. 41, no. 4, pp. 1445–1457, 2021.

[16] K. Park, Y. Choi, W. J. Choi, H.-Y. Ryu, and H. Kim, "LSTM-Based battery remaining useful life prediction with multi-channel charging profiles," *IEEE Access*, vol. 8, pp. 20786–20798, 2020.

[17] Z. Xue, Y. Zhang, C. Cheng, and G. Ma, "Remaining useful life prediction of lithium-ion batteries with adaptive unscented Kalman filter and optimized support vector regression," *Neurocomputing*, vol. 376, pp. 95–102, 2020.

[18] A. Guha and A. Patra, "State of health estimation of lithium-ion batteries using capacity fade and internal resistance growth models," *IEEE Trans. Transport. Electrific.*, vol. 4, no. 1, pp. 135–146, Mar. 2017.

[19] Y. Zheng, W. Gao, M. Ouyang, L. Lu, L. Zhou, and X. Han, "State-of-charge inconsistency estimation of lithium-ion battery pack using mean-difference model and extended Kalman filter," *J. Power Sources*, vol. 383, pp. 50–58, 2018.

[20] B. Saha, K. Goebel, and J. Christophersen, "Comparison of prognostic algorithms for estimating remaining useful life of batteries," *Trans. Inst. Meas. Control*, vol. 31, no. 3/4, pp. 293–308, 2009.

[21] S. Hochreiter and J. Schmidhuber, "Long short-term memory," *Neural Comput.*, vol. 9, no. 8, pp. 1735–1780, 1997.

[22] J. Qu, F. Liu, Y. Ma, and J. Fan, "A neural-network-based method for RUL prediction and SOH monitoring of lithium-ion battery," *IEEE Access*, vol. 7, pp. 87178–87191, 2019.

[23] L. Zhao, Y. Wang, and J. Cheng, "A hybrid method for remaining useful life estimation of lithium-ion battery with regeneration phenomena," *Appl. Sci.*, vol. 9, no. 9, p. 1890, 2019, doi: 10.3390/app9091890.

Yingzhou Wang was born in Shanxi, China, in 1987. He received the B.E. and M.E. degrees in control science and engineering from North China Electric Power University, Hebei, China, in 2011 and 2014, respectively, and the Ph.D. degree in power engineering from Northeast Electric Power University, Jilin, China, in 2021.

He is currently an Associate Professor with the School of Automation Engineering, Northeast Electric Power University. His research interests include state and life estimation, thermal effect, fault diagnosis of lithium-ion batteries in electrical vehicles, and energy storage.

Chenyang Hei was born in Liaoning, China, in 1998. He received the B.E. degree from Northeast Electric Power University, Jilin, China, in 2021. He is currently working toward the M.E. degree with Northeastern University, Shenyang, China.

His research interests include SD-WAN, intent-based networking, and cellular network configuration synthesis.

Hui Liu was born in Shandong, China, in 1975. He received the Ph.D. degree in electrical engineering from Tianjin University, Tianjin, China, in 2005.

He is currently the Vice President of the State Grid Jibei Electric Power Research Institute (North China Electric Power Research Institute Co. Ltd), Beijing, China. His research interests include renewable energy generation system, power system stability, VSC-HVdc, and grid-connected inverter control.

Shude Zhang (Student Member, IEEE) was born in Shandong, China, in 1995. He received the B.E. degree in automation, in 2018, from Northeast Electric Power University, Jilin, China, where he is currently working toward the Ph.D. degree in control science and engineering.

His research interests include state estimation and health management of lithium-ion batteries in electrical vehicles as well as energy storage systems.

Jianguo Wang was born in Jilin, China, in 1963. He received the B.S. and M.S. degrees in engineering from Tianjin University, Tianjin, China, in 1985 and 1988, respectively, and the Ph.D. degree from North China Electric Power University, Hebei, China, in 2001.

He is currently a Professor in automation engineering with Northeast Electric Power University, Jilin, China. His research interests include theory and technology of state intelligent diagnosis for power generating equipment, fouling monitoring of heat exchanger and its countermeasures, fault monitoring and diagnosis of wind turbine, and battery management system.